Microscopy at the Frontiers of Science 2017

mfs 2017

Zaragoza (Spain)
September 5th – 8th 2017

Abstract Book

SME SOCIEDAD DE MICROSCOPÍA DE ESPAÑA

Sociedade Portuguesa de Microscopia SPMicros

http://ina.unizar.es/mfs2017/

Low Energy Nuclear Techniques and Microscopy in Surface Analysis of Materials

J. A. R. Pacheco de Carvalho[1,2], C. F. R. Pacheco[2] and A. D. Reis[1,2]

[1.] Departamento de Física, Universidade da Beira Interior, Rua Marquês d'Ávila e Bolama, 6201-001 Covilhã, Portugal.
[2.] APTEL Research Group, Universidade da Beira Interior, Rua Marquês d'Ávila e Bolama, 6201-001 Covilhã, Portugal.

Techniques involving e.g. ion, electron and photon beams interacting with solid targets have been developed for surface analysis. The techniques give target information for depths near the surface. They are typically complementing. There exist both nuclear and non-nuclear techniques. Nuclear techniques, which are mainly non-destructive, permit investigations for a few microns close to the surface. Absolute values of concentrations of isotopes and elements are obtained. Their main applications have been scientific, technologic, in industry, arts, archaeology and medicine, using low energy MeV ion beams [1-6]. Nuclear reaction analysis permits detection of isotopes with high sensitivities. We use ion-ion reactions and the energy analysis method. At a competently chosen energy of the incident ion beam, an energy spectrum is recorded of ions from reaction events occurring at several depths in the target. Θ_L is the laboratory detection angle, and Θ_R is the target rotation angle. Such spectra are computer predicted and compared to experimental data, giving target composition and concentration profile information [4-7]. Elastic scattering is a special and important case. A computer program has been developed for flat targets [4-6]. The non-flat target case is an extension. Microscopy has been applied e.g. to material and life sciences. Potentialities of the method are illustrated by $^{18}O(p,\alpha_0)^{15}N$ and $^{12}C(d,p_0)^{13}C$ reactions and elastic scattering of $(^4He)^+$ ions, for three types of samples. SEM microscopy is used as a complementary technique for surface imaging.

Experimental details have been given [4]. Charged particle spectra were acquired from samples: 1) S1, a thick oxidized steel sample, prepared by high temperature oxidation of austenitic steel in $C^{18}O_2$ gas; weight gain data gave a 4.2 μm oxide thickness; a uniform step concentration profile of ^{18}O was anticipated; the oxide was satisfactorily flat. 2) S2, a thick pyrolitic graphite target, prepared by CH_4 cracking at 2200 ºC and deposition on a graphite substrate; the surface of the sample was plane. 3) S3, a thick flat sapphire sample (Al_2O_3); step concentration profiles of Al and O were foreseen.

Spectral data were obtained at $\Theta_L=165^o$ from: 1) S1, for $\Theta_R=0^o$, using the $^{18}O(p,\alpha_0)^{15}N$ reaction at E_p=1.78 MeV, an energy slightly above the resonance energy at 1.766 MeV in the differential cross section. 2) S2, using the $^{12}C(d,p_0)^{13}C$ reaction at E_d=1.40 MeV. 3) S3, for $\Theta_R=0^o$, using a $(^4He)^+$ ion beam at E_α=1.5 MeV. Published nuclear data, namely for reaction differential cross section and stopping power, were used in the computer predictions. For the $^{12}C(d,p_0)^{13}C$ reaction, reported differential cross-section data were used, as shown in Fig. 2 [4]. For elastic scattering, Rutherford differential cross-sections were included. Good fits were obtained. For S1, a uniform concentration profile of ^{18}O was found with X_1=4.4 μm (Fig. 1), close to the expectation. For S2, a probed depth with X_1=10 μm and uniform concentration of ^{12}C were found (Fig. 3). For S3, uniform step concentration profiles were found for Al and O with X_1=0.53 μm and X_1=0.23 μm, respectively (Fig. 4). The present work has shown high potentialities of the combined use of nuclear techniques and microscopy, as highly powerful analytical tools for non-destructive surface analysis of materials [8].

References:
[1] Y. Wang and M. Nastasi (eds.), "Handbook of Modern Ion Beam Materials Analysis", 2nd edition, (Materials Research Society, Pittsburgh, PA) (2009).
[2] G. Amsel and G. Battistig, Nucl. Instr. and Meth. B **240** (2005), 1-12.
[3] J. M. Calvert *et al,* J. Phys. D: Appl. Phys. **7** (1974), 940-953.
[4] J. A. R. Pacheco de Carvalho and A. D. Reis, Bol. Soc. Esp. Ceram. V. **47**, 4 (2008), 252-257.
[5] J. A. R. Pacheco de Carvalho and A. D. Reis, Nucl. Instr. and Meth. B **266**, 10 (2008), 2263-2267.
[6] J. Pacheco de Carvalho *et al,* Microsc. Microanal. **19**, S4 (2013), 133-134.
[7] N.P. Barradas *et al,* Nucl. Instr. and Meth. B **262** (2007), 281-303.
[8] Supports from Universidade da Beira Interior and FCT (Fundação para a Ciência e a Tecnologia)/PEst-OE-FIS/UI0524/2014 (Projecto Estratégico-UI524-2014) are acknowledged.

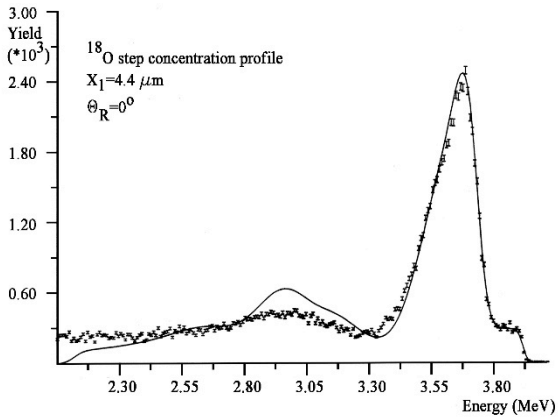

igure 1. Computed fit to the $^{18}O(p,\alpha_0)^{15}N$ reaction spectrum of the $C^{18}O_2$ oxidized steel target, S1, for E_p=1.78 MeV, Θ_L=165°.

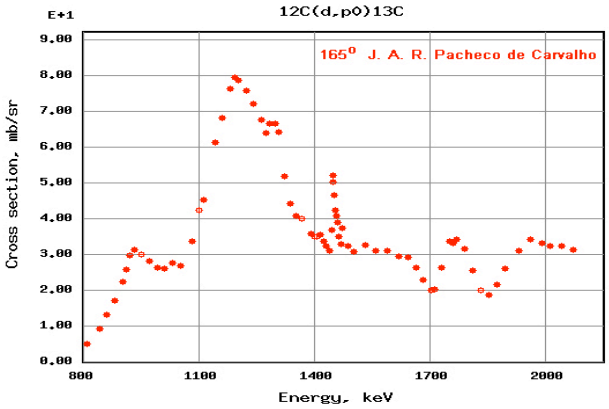

Figure 2. Differential cross section data of t $^{12}C(d,p_0)^{13}C$ reaction at Θ_L=165°.

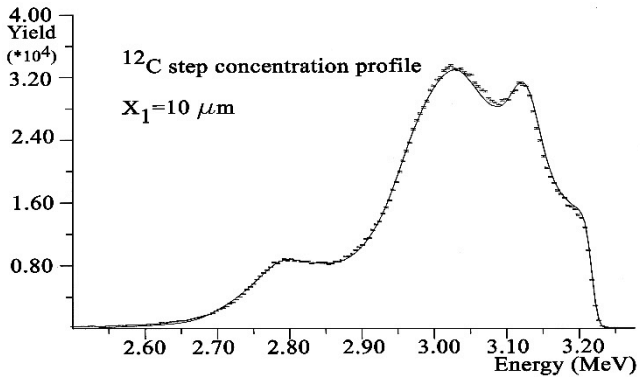

igure 3. Computed fit to the $^{12}C(d,p_0)^{13}C$ reactio data from the pyrolytic graphite target, S2, for E_d=1.40 MeV, Θ_L=165°.

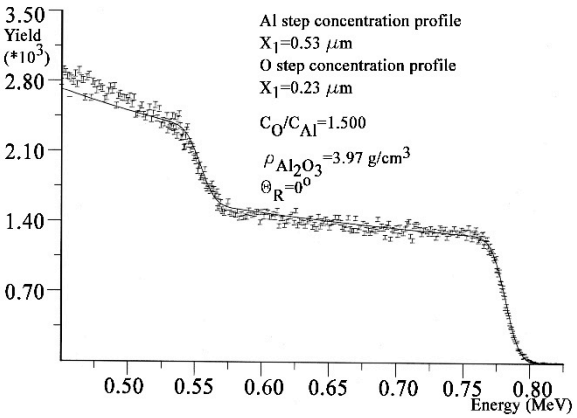

Figure 4. Computed fit to the elastic scattering spectrum from the sapphire target, S3, for E_α=1.5 MeV, Θ_L=165°.